Unusual Redox Behavior of α-Oligoheteroaromatic Compounds: An Increasing First Oxidation Potential with Increasing Conjugation Length

J. A. E. H. van Haare, L. Groenendaal, H. W. I. Peerlings, E. E. Havinga, J. A. J. M. Vekemans, R. A. J. Janssen,* and E. W. Meijer*

Laboratory of Organic Chemistry, Eindhoven University of Technology, PO Box 513, 5600 MB Eindhoven, The Netherlands

Received July 19, 1995[⊗]

Phenyl end-capped α-oligoheteroaromatic compounds consisting of pyrrole and thiophene units have been synthesized via Stille coupling reactions. Cyclic voltammetry studies on diphenyl-α-oligopyrroles (PhP_nPh) reveal two chemically reversible oxidation waves for $n \geq 2$, with decreasing potentials for larger n. For bis(phenylpyrrolyl)-α-oligothiophenes ($PhPT_nPPh$), in contrast, we observe an increase of the first and a decrease of the second oxidation potential going from $n = 1$ to $n = 3$. The bandgap in both series follows the usual decreasing behavior with increasing conjugation length. The oxidation potentials of both PhP_nPh and $PhPT_nPPh$ are explained using a Hückel-type band model. This theoretical model indicates that in the oxidized form of $PhPT_nPPh$, the positive charge tends to localize on the pyrrole units.

Introduction

Semiconducting polymers have been subject of considerable attention in recent years because of their interesting electrical and optical properties. A large family of π-conjugated polymers has been prepared with special prominence for homopolymers such as the poly(3-alkylthiophene)s, polypyrrole, polyphenylene, poly(*p*-phenylenevinylene)s, and polyaniline.[1] The preparation and properties of heteroaryl copolymers have received less attention.[2] Introducing structurally different units in a single π-conjugated polymer chain, however, may lead to new properties and add to the scope of applications for these materials. The recent development of novel low-bandgap polymers consisting of alternating structures of donor and acceptor moieties serves as an example for the new properties that can be obtained using π-conjugated copolymers.[3]

Many of the electronic and optical properties of π-conjugated polymers are related to their redox properties and have been associated with nonlinear soliton, polaron, and bipolaron excitations.[4] Conjugated oligomers with a well-defined chemical structure have been successfully used to assess optical and redox properties of semiconducting polymers in detail, especially in studying effects of (effective) conjugation length. Numerous experimental[5–9] and theoretical[10] studies on various π-conjugated homooligomers have shown that the energy of the $\pi-\pi^*$ transition as well as the first and second oxidation potentials decrease proportionally with the inverse number of double bonds when extending the π-conjugation. Detailed studies are available on the electronic structure of oligothiophene radical cations, radical cation π-dimers, and dications, being molecular analogues for polaronic and bipolaronic charge carriers in doped conjugated polymers.[5]

The redox properties of oligomers consisting of different aromatic rings have received little attention. Recently, Cava et al. have studied mixed thienylpyrrole

[⊗] Abstract published in *Advance ACS Abstracts,* September 15, 1995.

(1) See: Proceedings of the International Conference on Synthetic Metals 1994. *Synth. Met.* **1995**, *69–71*, 1–2304.

(2) (a) Reynolds, J. R.; Katritzky, A. R.; Soloducho, J.; Belyakov, S.; Sotzing, G. A.; Pyo, M. *Macromolecules* **1994**, *27*, 7225. (b) Röckel, H.; Gleiter, R.; Schuhmann, W. *Adv. Mater.* **1994**, *6*, 568. (c) Joshi, M. V.; Hemler, C.; Cava, M. P.; Cain, J. L.; Bakker, M. G.; McKinley, A. J.; Metzger, R. M. *J. Chem. Soc., Perkin Trans. 2* **1993**, 1081. (d) Martina, S.; Schlüter, A.-D. *Macromolecules* **1992**, *25*, 3607. (e) Zhou, Z.-H.; Maruyama, T.; Kanbara, T.; Ikeda, T.; Ichimura, K.; Yamamoto, T.; Tokuda, K. *J. Chem. Soc., Chem. Commun.* **1991**, 1210. (f) Ferraris, J. P.; Hanlon, T. R. *Polymer* **1989**, *30*, 1319. (g) Ferraris, J. P.; Andrus, R. G.; Hrncir, D. C. *J. Chem. Soc., Chem. Commun.* **1989**, 1318. (h) Pouwer, K. L.; Vries, T. R.; Havinga, E. E.; Meijer, E. W.; Wynberg, H. *J. Chem. Soc., Chem. Commun.* **1988**, 1432. (i) Inganäs, O.; Liedberg, B.; Chang-Ru, W.; Wynberg, H. *Synth. Met.* **1985**, *11*, 239. (j) Naitoh, S. *Synth. Met.* **1987**, *18*, 237.

(3) (a) Havinga, E. E.; ten Hoeve, W.; Wynberg, H. *Synth. Met.* **1993**, *55–57*, 299. (b) Tanaka, S.; Yamashita, Y. *Synth. Met.* **1993**, *55–57*, 1251. (c) Kitamura, C.; Tanaka, S.; Yamashita, Y. *J. Chem. Soc., Chem. Commun.* **1994**, 1585. (d) Tanaka, S.; Yamashita, Y. *Synth. Met.* **1995**, *69*, 599. (e) Ferraris, J. P.; Bravo, A.; Kim, W.; Hrncir, D. C. *J. Chem. Soc., Chem. Commun.* **1994**, 991.

(4) (a) Heeger, A. J.; Kivelson, S.; Schrieffer, J. R.; Su, W. P. *Rev. Mod. Phys.* **1988**, *60*, 781. (b) Lu, Y. *Solitons and Polarons in Conducting Polymers*; World Scientific: Singapore, 1988.

(5) (a) Hill, M. G.; Mann, K. R.; Miller, L. L.; Penneau, J.-F. *J. Am. Chem. Soc.* **1992**, *114*, 2728. (b) Bäuerle, P.; Segelbacher, U.; Maier, A.; Mehring, M. *J. Am. Chem. Soc.* **1993**, *115*, 10, 217. (c) Bäuerle, P.; Segelbacher, U.; Gaudl, K.-U.; Huttenlocher, D.; Mehring, M. *Angew. Chem., Int. Ed. Engl.* **1993**, *32*, 76. (d) Hapiot, P.; Audebert, P.; Monnier, K.; Pernaut, J.-M.; Garcia, P. *Chem. Mater.* **1994**, *6*, 1549. (e) Xu, Z.; Fichou, D.; Horowitz, G.; Garnier, F. *J. Electroanal. Chem.* **1989**, *267*, 339. (f) Garcia, P.; Pernaut, J.-M.; Hapiot, P.; Wintgens, V.; Valat, P.; Garnier, F.; Delabouglise, D. *J. Phys. Chem.* **1993**, *97*, 513. (g) Guay, J.; Kasai, P.; Diaz, A.; Wu, R.; Tour, J. M.; Dao, L. H. *Chem. Mater.* **1992**, *4*, 1097. (h) Zotti, G.; Schiavon, G.; Berlin, A.; Pagani, G. *Chem. Mater.* **1993**, *5*, 620. (i) Havinga, E. E.; Rotte, I.; Meijer, E. W.; Ten Hoeve, W.; Wynberg, H. *Synth. Met.* **1991**, *41–43*, 473. (j) Janssen, R. A. J.; Smilowitz, L.; Sariciftci, N. S.; Moses, D. *J. Chem. Phys.* **1994**, *101*, 1787. (k) Bäuerle, P.; Fischer, T.; Bidlingmeier, B.; Stabel, A.; Rabe, J. P. *Angew. Chem., Int. Ed. Engl.* **1995**, *34*, 303.

(6) Zotti, G.; Martina, S.; Wegner, G.; Schlüter, A.-D. *Adv. Mater.* **1992**, *4*, 798.

(7) (a) Meerholz, K.; Heinze, J. *J. Am. Chem. Soc.* **1989**, *111*, 2325. (b) Meerholz, K.; Heinze, J. *Angew. Chem.* **1990**, *102*, 695.

(8) Heinze, J.; Mortensen, J.; Müllen, K.; Schenk, R. *J. Chem. Soc., Chem. Commun.* **1987**, 701.

(9) Moll, T.; Heinze, J. *Synth. Met.* **1993**, *55–57*, 1521.

(10) Brédas, J. L.; Silbey, R.; Boudreaux, D. S.; Chance, R. R. *J. Am. Chem. Soc.* **1983**, *105*, 6555.

0897-4756/95/2807-1984$09.00/0

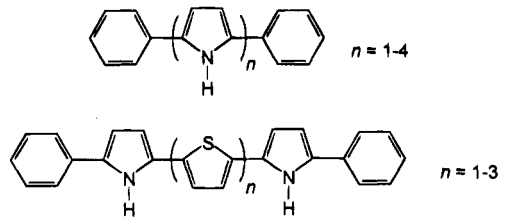

Figure 1. Molecular structures of PhP_nPh (**7a–d**) and $PhPT_n$-PPh (**8a–c**).

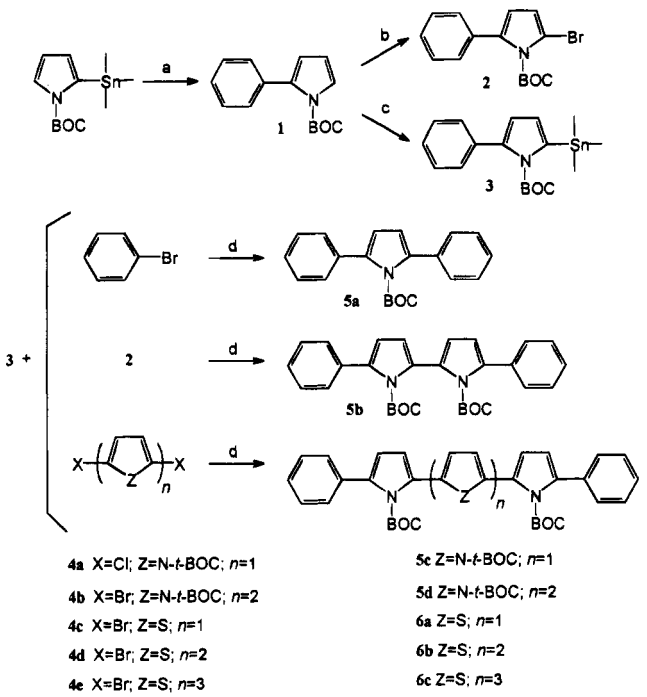

Figure 2. (a) PhBr; 2 mol% $Pd(PPh_3)_4$, toluene/water (1 M Na_2CO_3, 1:1 v/v), reflux, yield 80%; (b) NBS, THF, −70 °C, yield 100%; (c) (1) 2,2,6,6-tetramethylpiperidine, *n*-BuLi, THF, −70 °C, (2) $(CH_3)_3SnCl$, THF, −70 °C, yield 90%; (d) 2 mol % $Pd(PPh_3)_4$, toluene/water (1 M Na_2CO_3, 1:1 v/v), reflux.

oligomers up to seven units without reporting on particular properties deviating from homooligomers.[11] Here we report on the electrochemical properties of diphenyl-α-oligopyrroles (PhP_nPh, $n = 1-4$) and bis-(phenylpyrrolyl)-α-oligothiophenes ($PhPT_nPPh$, $n = 1-3$, Figure 1) and find a remarkable exception to the usual redox behavior of π-conjugated oligomers: The first oxidation potential ($E°_1$) of the $PhPT_nPPh$ oligomers increases with increasing conjugation length. In contrast, the second oxidation potential ($E°_2$) and the onset of the bandgap (E_g), exhibit the usual decreasing trend with larger *n*. This phenomenon is explained using a Hückel-type band model.

Results and Discussion

Synthesis. The synthetic route to *N*-(*tert*-butoxycarbonyl-protected PhP_nPh and $PhPT_nPPh$ oligomers is outlined in Figure 2. *N*-(*tert*-Butoxycarbonyl)-2-trimethylstannylpyrrole is reacted with bromobenzene in a palladium-catalyzed crossed-coupling reaction[12,13] to obtain *N*-(*tert*-butoxycarbonyl)-2-phenylpyrrole (**1**). Bromination of **1** provides **2**, while stannylation of **1** wth trimethyltin chloride affords the key intermediate *N*-(*tert*-butoxycarbonyl)-2-phenyl-5-(trimethylstannyl)pyrrole (**3**). Another Stille coupling reaction of **3** with either bromobenzene, **2**, or the α,α′-dihalogenoligopyrroles (**4a,b**) and α,α′-dihalogenoligothiophenes (**4c–e**) provides the *N*-*t*-BOC protected oligomers **5a–d** and **6a–c**.[14] After purification (extraction, column chromatography, crystallization) and characterization, the *N*-protecting *tert*-butoxycarbonyl groups are removed quantitatively by thermal treatment of the oligomers at 185 °C for 15 min under vacuum (evolution of isobutene and carbon dioxide). Complete deprotection was checked using ^1H NMR spectroscopy and is also apparent from the bathochromic shift of the electronic $\pi-\pi^*$ absorption. The bathochromic shift for the oligomers is the result of the higher degree of coplanarity of the aromatic units that can be achieved when the *N*-*t*-BOC group is replaced by a sterically less demanding hydrogen atom. The solubility of the oligomers decreases significantly upon deprotection.

Table 1. Electrochemical Data[a] and Onset of $\pi-\pi^*$ Absorption[b]

oligomer	E_{pa1} (V)	E_{pc1} (V)	E_{pa2} (V)	E_{pc2} (V)	E_g (eV)
PhPPh	*c*				3.44
PhP_2Ph	0.42	0.33	1.09	1.00	3.05
PhP_3Ph	0.16	0.10	0.64	0.57	2.89
PhP_4Ph	0.06	−0.04	0.43	0.32	2.78
PhPTPPh	0.47	0.36	0.86	0.75	2.72
$PhPT_2PPh$	0.54	0.43	0.70	0.60	2.52
$PhPT_3PPh$[d]	0.66	0.55	0.66	0.55	2.39

[a] Potentials in $CH_2Cl_2/Bu_4N^+PF_6^-$ (0.1 M) vs SCE, oligomer concentration $c = 0.5-10$ mM. [b] Absorption spectra recorded in acetonitrile. [c] Irreversible oxidation wave. [d] A broad oxidation wave is observed, assigned to a coalescence of E_{pa1} and E_{pa2}.

Optical and Redox Properties. The UV/vis absorption spectra of both PhP_nPh and $PhPT_nPPh$ reveal that the onset of the $\pi-\pi^*$ transition (E_g, Table 1) shifts to lower energies with increasing number of rings, consistent with the expected behavior for increasing π-conjugation. Figure 3 shows that both series exhibit approximately a linear behavior of E_g as a function of the inverse conjugation length of the oligomer which is taken as $1/m$, where *m* corresponds to the total number of aromatic rings in the oligomer.

Using cyclic voltammetry, we find that PhP_nPh oligomers exhibit two chemically reversible oxidation waves for $n \geq 2$ (Figure 4a). For $n = 1$, polymerization occurs, resulting in a dark-red film on the working electrode. The chemical stability of PhP_nPh monocation radicals and dications is significantly enhanced as compared to P_n.[6] Chemically reversible one-electron oxidation for P_n has been observed starting at $n = 3$ for scan rates over 1000 mV/s, while the second one-electron oxidation wave becomes reversible at $n = 5$.[6] As expected for π-conjugated oligomers, $E°_1$ and $E°_2$ of PhP_nPh decrease approximately linearly with the reciprocal number of rings (Figure 5).

(11) (a) Niziurski-Mann, R. E.; Scordillis-Kelly, C.; Liu, T.-L.; Cava, M. P.; Carin, R. T. *J. Am. Chem. Soc.* **1993**, *115*, 887. (b) Niziurski-Mann, R. E.; Cava, M. P. *Adv. Mater.* **1993**, *5*, 547. (c) Cava, M. P.; Parakka, J. P.; Lakshmikantham, M. V. *Mater. Res. Soc., Symp. Proc.* **1994**, *328*, 179. (d) Parakka, J. P.; Cava, M. P. *Synth. Met.* **1995**, *68*, 275.

(12) Stille, J. K. *Angew. Chem., Int. Ed. Engl.* **1986**, *25*, 508.

(13) (a) Martina, S.; Enkelmann, V.; Schlüter, A.-D.; Wegner, G. *Synth. Met.* **1991**, *41–43*, 403. (b) Martina, S.; Enkelmann, V.; Schlüter, A.-D.; Wegner, G. *Synthesis* **1991**, *41–43*, 613. (c) Martina, S.; Enkelmann, V.; Wegner, G.; Schlüter, A.-D. *Synth. Met.* **1991**, *41–43*, 403.

(14) Groenendaal, L.; Peerlings, H. W. I.; Havinga, E. E.; Vekemans, J. A. J. M.; Meijer, E. W. *Synth. Met.* **1995**, *69*, 467.

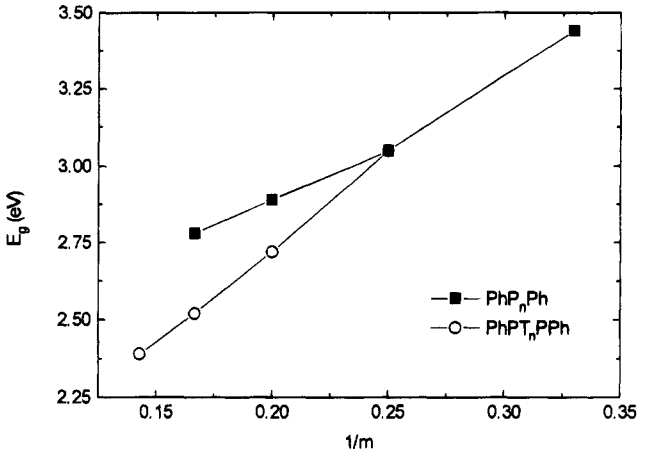

Figure 3. Onset of the $\pi-\pi^*$ transition of the PhP_nPh and $PhPT_nPPh$ oligomers in acetonitrile solution vs inverse conjugation length ($1/m$; m being the total number of aromatic rings in the oligomer).

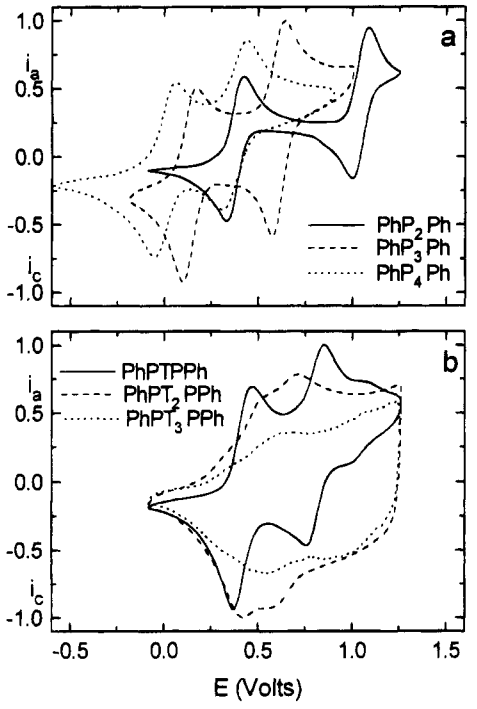

Figure 4. Cyclic voltammograms of PhP_nPh (a) and $PhPT_nPPh$ (b) in $CH_2Cl_2/NBu_4^+PF_6^-$ (0.1 M) solution, scanned at 100 mV/s. Potential vs SCE, internally calibrated vs Fc/Fc^+.

The redox behavior of the $PhPT_nPPh$ series is dramatically different from that of the PhP_nPh oligomers. In Figure 4b we show that the first oxidation wave for $PhPT_nPPh$ occurs at a higher potential as compared to PhP_2Ph, despite a longer conjugation length and a decreased onset of the $\pi-\pi^*$ transition. Further incrementing the number of thiophene rings between the two pyrrole rings results in a steady increase of $E°_1$ (Figure 5), while $E°_2$ continues to decrease. For $PhPT_3PPh$ first and second oxidation potentials coalesce into a single broad oxidation wave.

Hückel-Type Band Model. The different redox behavior of PhP_nPh and $PhPT_nPPh$ with increasing n can be described using an elementary Hückel-type band model in which each pyrrole, thiophene, and benzene ring is represented by one doubly occupied level. The doubly occupied ring energy levels are combined into a band structure using a standard Hückel-type calculation

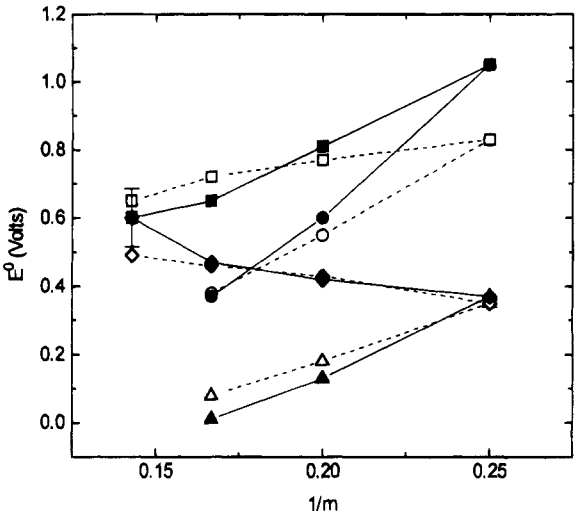

Figure 5. First and second oxidation potentials (vs SCE) as function of inverse conjugation length ($1/m$) for PhP_nPh ($m = n + 2$, ▲ and ●) and $PhPT_nPPh$ ($m = n + 4$, ◆ and ■). Closed markers refer to experimental data; open markers to calculated values using Hückel band model.

with Hückel parameters $\alpha_P = -1.26$ eV for pyrrole, $\alpha_T = -2.00$ eV for thiophene, and $\alpha_{Ph} = -2.50$ eV for benzene. The α values are approximately linearly dependent on the experimental ionization potential (pyrrole 8.2 eV; thiophene 8.86 eV; benzene 9.24 eV).[15] The interaction between the rings in this model is represented by a single common β value ($\beta_{PP} = \beta_{TP} = \beta_{TT} = \beta_{PPh} = -0.69$ eV) for all nearest-neighbor interactions and taken to be zero otherwise. The calculated oxidation potential in our model is $-\epsilon_n$, where ϵ_n is the energy of the highest level. Using only these four parameters, we were able to fit 19 different experimental first oxidation potentials for oligothiophenes,[5e] oligopyrroles,[6] and mixed oligoheterocycles with a root-mean-square (rms) error of 0.038 V (Table 2). A slightly better fit (rms error 0.033 V) could be obtained when separate β values were used for each type of ring–ring interaction.

The second oxidation potential, $E°_2$, differs in a first approximation from $E°_1$ by the electron–electron repulsion integral J_{nn} associated with the highest level. J_{nn} can be estimated in zeroth order from the corresponding Hückel expansion coefficients and a one-ring repulsion integral γ using the relation $J_{nn} = \gamma\Sigma c^4$. Again, a single γ value is taken to represent the electron–electron repulsion in pyrrole, thiophene, and benzene rings. The rms error for the second oxidation potential calculated from $-\epsilon_n + J_{nn}$ using $\gamma = 1.15$ eV is 0.095 V over 12 experimental values (Table 2).

Using this Hückel model, we find an excellent agreement between the calculated ionization potential and the experimental values for $E°_1$ of PhP_nPh, whereas the difference between $E°_2$ and $E°_1$ for PhP_nPh can be reproduced reasonably well (Figure 5). More important for the present study, we find that the increasing first oxidation potential and decreasing second oxidation potential for the $PhPT_nPPh$ oligomers are reproduced by this model (Figure 5). Although, in principle, both electrons are removed from the same molecular orbital,

(15) Weast, R. C., Ed. *CRC Handbook of Chemistry and Physics*, 60th ed.; Chemical Rubber Publishing Company: Boca Raton, FL, 1980; pp E75–81.

Table 2. Calculated and Experimental Oxidation Potentials[a]

	$E°_1$(calc)	$E°_1$(obs)	Δ_1	$E°_2$(calc)	$E°_2$(obs)	Δ_2
PhPPh	0.72			1.43		
PhPPhPPh	0.53	0.69	−0.06	0.88	0.90	−0.02
PhP_2Ph	0.35	0.37	−0.02	0.83	1.05	−0.21
PhP_3Ph	0.18	0.13	+0.05	0.55	0.60	−0.05
PhP_4Ph	0.08	0.01	+0.07	0.38	0.37	+0.01
PhPTPh	0.60	0.67	+0.07	1.16	1.36	−0.20
PhPTPPh	0.43	0.42	+0.01	0.77	0.81	−0.04
$PhPT_2PPh$	0.46	0.47	−0.01	0.72	0.65	+0.07
$PhPT_3PPh$	0.49	~0.60		0.71	~0.60	
PhPTPTPPh	0.32	0.31	+0.01	0.57	0.53	+0.04
T	2.00	1.97	+0.03	3.15		
T_2	1.31	1.27	+0.04	1.89		
T_3	1.02	1.00	+0.02	1.45		
T_4	0.88	0.90	−0.02	1.23		
T_5	0.81	0.84	−0.03	1.10		
T_6	0.76	0.79	−0.03	1.01		
P_1	1.26	1.31	−0.05	2.41		
P_2	0.57	0.58	−0.01	1.15		
P_3	0.28	0.23	+0.05	0.71	0.80	−0.09
P_4	0.14			0.49		
P_5	0.06	0.07	−0.01	0.35	0.27	+0.08
P_6	0.02			0.27		
P_7	−0.02	0.00	−0.02	0.20	0.10	+0.10

[a] Experimental data for P_n are taken from ref 6 and corrected with +0.35 V to convert to SCE. Data for T_n are from ref 5e and corrected with −0.05 V to allow for a reasonable estimate for the difference between E_{pa} and $E°$.

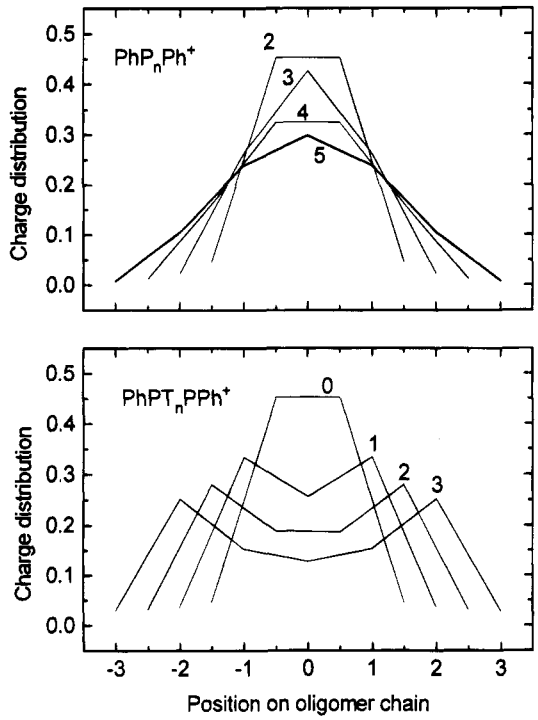

Figure 6. Calculated charge distribution for PhP_nPh^+ and $PhPT_nPPh^+$ radical cations using Hückel band model. The numbers in the graph refer to n.

the stabilization due to loss of electron−electron repulsion energy in a one-electron oxidation is larger for short oligomers than for longer oligomers, explaining the different trend for $E°_1$ and $E°_2$ with increasing n. Compared to PhP_nPh, the calculated charge distribution of $PhPT_nPPh$ radical cations is shifted from the central rings in the oligomer toward the pyrrole rings (Figure 6). In fact, the highest positive charge density of $PhPT_nPPh$ radical cations is predicted to reside on the two pyrrole rings. The band calculations for $PhPT_nPPh$ reveal that the two highest doubly occupied levels quickly become degenerate with increasing n, converging toward the value of $\epsilon = -0.53$ eV for $PhPT_n$ in the $n = \infty$ limit. This near degeneracy of the highest levels has an important consequence for calculating the second oxidation potential. For $PhPT_3PPh$, the calculated loss of repulsion energy in the first oxidation step (J_{nn}), is larger than the energy difference between the highest and penultimate levels. Hence, the values for $E°_2$ of $PhPT_nPPh$ shown in Figure 5 are determined from $E°_1 + J_{nn}$ for $n \leq 2$ and taken from the penultimate level for $n = 3$.

Concluding Remarks

In conclusion, we find that the redox properties of mixed oligomers of pyrrole, thiophene, and benzene rings exhibit a behavior very different from that of typical conjugated homooligomers and that the actual sequence of the different monomers in a π-conjugated chain is important to the redox potential. We find a good agreement between the experimental oxidation potentials and those obtained from an elementary model using a minimum of four parameters. The model explains the unusual observation that the first oxidation potential increases for $PhPT_nPPh$ with increasing n.

Experimental Section

General Techniques. All solvents and reagents were reagent grade and used as received. Tetrahydrofuran (THF) was distilled over Na/benzophenone. For column chromatography Merck silica gel 60 (particle size 0.063−0.200 mm) and Merck aluminum oxide 90 (neutral; activity I, deactivated with 7 wt % of water) were used. NMR spectra were recorded on a Bruker AM-400 spectrometer at frequencies of 400.1 and 100.6 MHz for ^1H and ^{13}C nuclei, respectively. Tetramethylsilane (TMS) or THF-d_8 was used as an internal standard for ^1H NMR and $CDCl_3$ for ^{13}C NMR. UV/vis spectra were recorded on a Perkin-Elmer Lambda 3B UV/vis spectrophotometer between 190 and 900 nm. Infrared (FT-IR) spectra were recorded on a Perkin-Elmer 1605 FT-IR spectrophotometer between 4400 and 450 cm^{-1}. All experiments on deprotected oligomers were conducted under rigorously inert conditions (water < 1 ppm; oxygen < 3 ppm). Cyclic voltammograms were obtained in dichloromethane with 0.1 M tetrabutylammonium hexafluorophosphate ($Bu_4N^+PF_6^-$) as supporting electrolyte using a Potentioscan Wenking POS73 potentiostat. A platinum disk (diameter 5 mm) was used as working electrode, the counter electrode was a platinum plate (5 × 5 mm^2), and a saturated calomel electrode (SCE) was used as reference electrode, internally calibrated vs Fc/Fc^+.

***N*-(*tert*-Butoxycarbonyl)-2-phenylpyrrole (1).** To bromobenzene (3.15 g, 20.00 mmol), dissolved in a mixture of toluene (30 mL) and a sodium carbonate (Na_2CO_3) solution (1 M in water, 30 mL), *N*-*tert*-butoxycarbonyl-2-(trimethylstannyl)-pyrrole[13b] (6.62 g, 20.00 mmol) was added. Upon deaeration and blanketing by argon, tetrakis(triphenylphosphine)palladium(0) ($Pd(PPh_3)_4$, 0.46 g, 0.40 mmol, 2 mol %) was added. After heating under reflux for 2 days, the mixture was allowed to cool to room temperature. The organic and aqueous layers were separated, and the aqueous layer was extracted with diethyl ether (3 × 20 mL). The organic layers were combined, dried ($MgSO_4$), and concentrated. Column chromatography (300 g of SiO_2; dichloromethane (CH_2Cl_2):hexane (1:2); R_f = 0.40) afforded pure **1** (3.91 g, 16.10 mmol, 80%) as a slightly purple oil. ^1H NMR ($CDCl_3$) δ 7.38−7.26 (m, 6H, PhH, H-5); 6.22 (t, J = 3.4 Hz, 1H, H-4); 6.18 (dd, J = 3.4 and 1.8 Hz, 1H, H-3); 1.33 (s, 9H, CH_3). ^{13}C NMR ($CDCl_3$) δ 149.0 (C=O); 135.0, 134.4 (C-2/ipso-Ph); 129.1, 127.5 (*o*-Ph/*m*-Ph); 127.1 (*p*-Ph); 122.5 (C-5); 114.3, 110.5 (C-3/C-4); 83.4 ($C-CH_3$); 27.5 (CH_3).

***N*-(*tert*-Butoxycarbonyl)-2-bromo-5-phenylpyrrole (2).** A solution of **1** (1.04 g, 4.30 mmol) in THF (20 mL) was cooled

to −70 °C under continuous stirring. *N*-Bromosuccinimide (0.76 g, 4.30 mmol) was added in portions, and stirring was continued for 30 min at −70 °C. The reaction mixture was stored at 4 °C overnight, and then Na_2SO_3 (0.20 g, 1.60 mmol) was added under vigorous stirring. After 30 min the reaction mixture was concentrated and the residue was taken up in CCl_4 (20 mL). The resulting suspension was filtered and the filtrate concentrated yielding pure **2** (1.38 g, 4.30 mmol, 100%) as a reddish oil. ^{1}H NMR ($CDCl_3$) δ 7.37−7.24 (m, 5H, PhH); 6.30 (d, J = 3.4 Hz, 1H, H-3); 6.16 (d, J = 3.4 Hz, 1H, H-4); 1.30 (s, 9H, CH_3). ^{13}C NMR ($CDCl_3$) δ 148.5 (C=O); 136.6, 134.0 (C-5/ipso-Ph); 128.1, 127.9 (*o*-Ph/*m*-Ph); 127.3 (*p*-Ph); 114.9, 112.6 (C-3/C-4); 101.9 (C-2); 84.9 (*C*−CH_3); 27.2 (CH_3).

***N*-(*tert*-Butoxycarbonyl)-2-phenyl-5-(trimethylstannyl)-pyrrole (3).** A solution of 2,2,6,6-tetramethylpiperidine (1.31 g, 9.39 mmol) in THF (25 mL) was cooled to −70 °C and blanketed by argon. *n*-Butyllithium in *n*-hexane (6.1 mL, 1.6 M, 9.80 mmol) was added dropwise, and the solution was stirred for 1 h at −70 °C and 30 min at room temperature. The mixture was then cooled to −70 °C and gradually treated with a solution of **1** (2.14 g, 8.80 mmol) in THF (5 mL) and stirred for 90 min at −70 °C. Finally, a solution of trimethyltin chloride (1.97 g, 9.90 mmol) in THF (5 mL) was added dropwise. Stirring was continued for 4 h at −70 °C and subsequently overnight at room temperature. The reaction mixture was concentrated, and diethyl ether (30 mL) and water (30 mL) were added to the residue. The organic and aqueous layers were separated and the aqueous layer was extracted with diethyl ether (2 × 20 mL). After drying of the combined organic extracts ($MgSO_4$), filtration, and concentration, **3** was obtained as 90% pure product which can be used directly for coupling reactions. Column chromatography (75 g Al_2O_3; hexane; R_f = 0.45) afforded pure **3** (1.55 g, 3.80 mmol) as a colorless oil. ^{1}H NMR ($CDCl_3$) δ 7.35−7.23 (m, 5H, PhH); 6.38 (d, J = 3.1 Hz, 1H, H-4); 6.27 (d, J = 3.1 Hz, 1H, H-3); 1.18 (s, 9H, CH_3); 0.30 (s, 9H, $Sn(CH_3)_3$); 0.30 (d, J_{SnH} = 32.0 Hz, $^{117}Sn(CH_3)_3$); 0.30 (d, J_{SnH} = 32.2 Hz, $^{119}Sn(CH_3)_3$). ^{13}C NMR ($CDCl_3$) δ 151.5 (C=O); 138.2, 137.6, 135.9 (C-2/C-5/ipso-Ph); 128.0, 127.5 (*o*-Ph/*m*-Ph); 126.8 (*p*-Ph); 121.4 (C-4); 115.4 (C-3); 83.3 (*C*−CH_3); 27.2 (C−*C*H_3); −7.5 ($Sn(CH_3)_3$).

***N*-(*tert*-Butoxycarbonyl)-2,5-dichloropyrrole (4a).** A solution of *N*-*tert*-butoxycarbonylpyrrole[13b] (1.67 g, 10.00 mmol) in THF (50 mL) was cooled to −70 °C and blanketed by argon. *N*-Chlorosuccinimide (2.94 g, 22.00 mmol) was added in portions, and the mixture was stirred for 1 h at −70 °C and then allowed to reach room temperature. After stirring for 12 h at room temperature, Na_2SO_3 (0.50 g, 4.00 mmol) was added to the white, turbid liquid, and the solvent was evaporated. The residue was treated with CCl_4 (50 mL), and the suspension was stirred for 15 min. Filtration and evaporation of the filtrate resulted in an orange liquid. After column chromatography (50 g SiO_2, CH_2Cl_2:hexane (1:3), R_f = 0.30), **4** was obtained as a colorless liquid (0.98 g, 4.20 mmol, 42%). ^{1}H NMR ($CDCl_3$) δ 6.08 (s, 2H, H-3,4); 1.63 (s, 9H, CH_3). ^{13}C NMR ($CDCl_3$) δ 146.7 (C=O); 115.9 (C−Cl); 110.6 (C-3,4); 86.1 (*C*−CH_3); 27.8 (CH_3).

***N*-(*tert*-Butoxycarbonyl)-2,5-diphenylpyrrole (5a).** Stille coupling of bromobenzene (0.71 g, 4.50 mmol) with **3** (1.83 g, 4.50 mmol) in toluene (25 mL) and Na_2CO_3 solution (1 M in water, 25 mL), catalyzed by $Pd(PPh_3)_4$, was performed as described for the preparation of **1**. Column chromatography (40 g SiO_2, hexane:CH_2Cl_2 (2:1), R_f = 0.49) and subsequent crystallization from ethanol afforded pure **5** (0.50 g, 1.6 mmol, 35%) as a white, crystalline solid, mp 120 °C. ^{1}H NMR ($CDCl_3$) δ 7.43−7.28 (m, 10H, PhH); 6.23 (s, 2H, H-3,4); 1.17 (s, 9H, CH_3). ^{13}C NMR ($CDCl_3$) δ 149.8 (C=O); 136.2, 134.1 (C-2,5/ipso-Ph); 128.8, 127.8 (*o*-Ph/*m*-Ph); 127.2 (*p*-Ph); 112.1 (C-3/C-4); 83.9 (*C*-CH_3); 27.1 (CH_3). UV (CH_3CN) λ_{max} 225, 290 nm. IR (KBr) ν 3073−2933, 1746, 1605, 1486, 1444, 1305, 1146, 643−701 cm^{-1}.

***N,N*'-Bis(*tert*-butoxycarbonyl)-5,5'-diphenyl-2,2'-bipyrrole (5b).** Stille coupling between **2** (0.310 g, 0.96 mmol) and **3** (0.408 g, 1.00 mmol) in toluene (6 mL) and Na_2CO_3 solution (1 M in water, 6 mL), catalyzed by $Pd(PPh_3)_4$, was performed as for the preparation of **1**. After workup a dark oil was obtained. Purification by column chromatography (15 g of SiO_2, CH_2Cl_2:hexane (1:1), R_f = 0.28) resulted in pure **6** (0.25 g, 0.25 mmol, 54%). ^{1}H NMR ($CDCl_3$) δ 7.38−7.28 (m, 10H, PhH); 6.27 (d, J = 3.4 Hz, 2H, H-3,3'/H-4,4'); 6.24 (d, J = 3.4 Hz, 2H, H-3,3'/H-4,4'); 1.25 (s, 18H, CH_3). ^{13}C NMR ($CDCl_3$) δ 149.3 (C=O); 136.6, 134.6 (C-5,5'/ipso-Ph); 128.4, 128.1 (*o*-Ph/*m*-Ph); 128.1 (C-2,2'); 127.0 (*p*-Ph); 114.4, 112.6 (C-4,4'/C-3,3'); 83.4 (*C*−CH_3), 27.4 (CH_3). UV (CH_3CN) λ_{max} 295 nm. This compound can also be obtained by performing an Ullmann coupling using **2** and copper bronze in DMF at 100 °C.[16]

***N,N',N''*-Tris(*tert*-butoxycarbonyl)-5,5''-diphenyl-2,2':5',2''-terpyrrole (5c).** Stille coupling between **3** (0.218 g, 0.54 mmol) and **4a** (0.060 g, 0.25 mmol) in toluene (1 mL) and Na_2CO_3 solution (1 M in water, 1 mL), catalyzed by $Pd(PPh_3)_4$, was performed as described for the preparation of **1**. After workup a dark green solid was obtained which was purified by column chromatography (10 g of SiO_2, CH_2Cl_2:hexane (1:1), R_f = 0.20) to afford pure **5c** (70 mg, 0.11 mmol, 43%). ^{1}H NMR ($CDCl_3$) δ 7.40−7.30 (m, 10H, PhH); 6.28 (s, 2H, H-3',4'); 6.26 (d, J = 3.4 Hz, 2H, H-3,3'/H-4,4'); 6.23 (d, J = 3.4 Hz, 2H, H-3,3'/H-4,4'); 1.34 (s, 9H, CH_3(BOC')); 1.26 (s, 18H, CH_3(BOC, BOC'')). ^{13}C NMR ($CDCl_3$) δ 149.2 (C=O (BOC, BOC'')); 149.0 (C=O (BOC')); 136.5, 134.7 (C-5,5''/ipso-Ph); 128.7, 127.7 (C-2,2''/C-2',5'); 128.3, 127.8 (*o*-Ph/*m*-Ph); 126.9 (*p*-Ph); 114.2, 114.1, 112.8 (C-3,3''/C-4,4''/C-3',4'); 83.3 (*C*-CH_3(BOC, BOC'')); 82.8 (*C*−CH_3(BOC')); 27.6 (CH_3(BOC')); 27.4 (CH_3(BOC,BOC'')). UV (CH_3CN) λ_{max} 301 nm.

***N,N',N'',N'''*-Tetrakis(*tert*-butoxycarbonyl)-5,5'''-diphenyl-2,2':5',2'':5'',2'''-quaterpyrrole (5d).** Stille coupling between **3** (0.13 g, 0.31 mmol) and *N,N'*-bis(*tert*-butoxycarbonyl)-5,5'-dibromo-2,2'-bipyrrole (**4b**,[16] 70 mg, 0.14 mmol) in toluene (2 mL) and Na_2CO_3 solution (1 M in water, 2 mL), catalyzed by $Pd(PPh_3)_4$, was performed as described for the preparation of **1**. The crude dark oil was purified by column chromatography (10 g SiO_2, CH_2Cl_2:hexane (1:1), R_f = 0.10) and afforded pure **5d** as a slightly brown solid (45 mg, 0.06 mmol, 39%). ^{1}H NMR ($CDCl_3$) δ 7.28−7.26 (m, 10H, PhH); 6.26 (d, J = 3.3 Hz, 2H, H-3,3'''/H-4,4'''); 6.22 (s, 4H, H-3',4',3'',4''); 6.19 (d, J = 3.3 Hz, 2H, H-3,3'''/H-4,4'''); 1.29, 1.24 (s, 36H, CH_3). ^{13}C NMR ($CDCl_3$) δ 149.3, 148.9 (C=O); 136.4, 134.8 (C-5,5'''/ipso-Ph); 128.8, 128.4, 128.3, 127.7, 127.6, 126.9 (*o*-Ph/*m*-Ph/*p*-Ph/C-2,2'/C-5',2''/C-5'',2'''); 114.4, 113.9, 113.8, 112.7 (C-3,3'''/C-4,4'''/C-3',3''/C-4',4''); 83.2, 82.8 (*C*−CH_3); 27.7, 27.4 (CH_3). UV (CH_3CN) λ_{max} 299 nm.

2,5-Bis(*N*-*tert*-butoxycarbonyl-5-phenyl-2-pyrrolyl)thiophene (6a). Stille coupling between **3** (0.408 g, 1.01 mmol) and 2,5-dibromothiophene (**4c**, 0.122 g, 0.51 mmol) in toluene (2 mL) and Na_2CO_3 solution (1 M in water, 2 mL), catalyzed by $Pd(PPh_3)_4$, was performed as described for the preparation of **1**. Column chromatography of the residue (40 g of SiO_2, hexane:CH_2Cl_2 (1:1), R_f = 0.43) gave pure **6a** (0.044 g, 0.10 mmol, 20%) as a red-brown, glassy compound. ^{1}H NMR ($CDCl_3$) δ 7.41−7.28 (m, 10 H, PhH); 7.07 (s, 2H, ThH-3,4); 6.38 (d, J = 3.5 Hz, 4H, PyH-3/PyH-4); 6.24 (d, J = 3.5 Hz, 4H, PyH-3/PyH-4); 1.25 (s, 18H, CH_3). ^{13}C NMR ($CDCl_3$) δ 149.6 (C=O); 136.7, 134.4, 134.0 (ThC-2/PyC-5/ipso-Ph); 128.4, 127.9 (*o*-Ph/*m*-Ph); 127.8, 127.2, 127.0 (ThC-3/*p*-Ph/PyC-2); 113.9, 112.1 (PyC-3/PyC-4); 83.4 (*C*−CH_3); 27.1 (CH_3). UV (CH_3CN) λ_{max} 331 nm. IR (KBr) ν 2977, 1750, 1302, 1141, 842−698 cm^{-1}.

5,5'-Bis(*N*-*tert*-butoxycarbonyl-5-phenyl-2-pyrrolyl)-2,2'-bithiophene (6b). Stille coupling between 5,5'-dibromo-2,2'-bithiophene (**4d**,[17] 0.150 g, 0.47 mmol) and **3** (0.427 g, 1.05 mmol) in toluene (8 mL) and Na_2CO_3 solution (1 M in water, 8 mL), catalyzed by $Pd(PPh_3)_4$, was performed as described for the prepartion of **1**. The crude residue was subjected to column chromatography (40 g of SiO_2, hexane:CH_2Cl_2 (1:1), R_f = 0.27) and subsequent crystallization yielded pure **6b** (75 mg, 0.12 mmol, 24 %) as a brown crystalline solid, mp 159 °C.

(16) (a) Groenendaal, L.; Peerlings, H. W. I.; Van Dongen, J. L. J.; Havinga, E. E.; Vekemans, J. A. J. M.; Meijer, E. W. *Polym. Prepr.* **1994**, *35*, 194. (b) Groenendaal, L.; Peerlings, H. W. I.; Van Dongen, J. L. J.; Havinga, E. E.; Vekemans, J. A. J. M.; Meijer, E. W. *Macromolecules* **1995**, *28*, 116.

(17) Bäuerle, P.; Würther, F.; Götz, G.; Effenberger, F. *Synthesis* **1993**, *11*, 1099−1103.

^{1}H NMR ($CDCl_3$) δ 7.41−7.30 (m, 10H, PhH); 7.12 (d, J = 3.7 Hz, 4H, ThH-3/ThH-4); 7.04 (d, J = 3.7 Hz, 4H ThH-3/ThH-4); 6.39 (d, J = 3.5, 4H, PyH-3/PyH-4); 6.25 (d, J = 3.5, 4H, PyH-3/PyH-4); 1.24 (s, 18H, CH_3). ^{13}C NMR ($CDCl_3$) δ 149.6 (C=O); 137.2, 137.1, 137.0, 134.0, 133.4 (ThC-2/ThC-5/PyC-2/PyC-5/ipso-Ph); 128.4, 128.2, 128.0 (ThC-4/*o*-Ph/*m*-Ph); 127.3 (*p*-Ph); 123.3 (ThC-3); 114.1, 112.1 (PyC-3,4); 84.4 (C−CH_3); 27.2 (CH_3). UV (CH_3CN) λ_{max} 364 nm. IR (KBr) ν 2978, 1751, 1295, 841−698 cm^{-1}.

5,5″-Bis(*N-tert*-butoxycarbonyl-5-phenyl-2-pyrrolyl)-2,2′:5′,2″-terthiophene (6c). Stille coupling between **3** (0.33 g, 0.81 mmol) and 5,5″-dibromo-2,2′:5′,2″-terthiophene (**4e**,[17] 0.16 g, 0.40 mmol) in toluene (2 mL) and Na_2CO_3 solution (1 M in water, 2 mL), catalyzed by $Pd(PPh_3)_4$, was performed as described for the preparation of **1**. After workup and column chromatography (20 g of SiO_2, EtOAc:hexane (1:9), R_f = 0.30), pure **6c** (60 mg, 0.08 mmol, 21%) was isolated. ^{1}H NMR ($CDCl_3$) δ 7.40−7.29 (m, 10H, PhH); 7.11 (d, J = 3.7 Hz, 2H, ThH-3,3″/ThH-4,4″); 7.08 (s, 2H, ThH-3′,4′); 7.05 (d, J = 3.7 Hz, 2H, ThH-3,3″/ThH-4,4″); 6.39 (d, J = 3.5 Hz, 2H, PyH-3/PyH-4); 6.24 (d, J = 3.5 Hz, 2H, PyH-3/PyH-4); 1.24 (s, 18H, CH_3). ^{13}C NMR ($CDCl_3$) δ 149.0 (C=O); 134.1, 130.9 (ipso-Ph/PyC-5); 128.8, 128.7, 127.9, 127.4, 127.1 (PyC-2/ThC-4/ThC-3/ThC-3′/*p*-Ph); 124.4, 124.2, 123.4 (ThC-5/ThC-2/ThC-2′); 128.5, 128.1 (*o*-Ph/*m*-Ph); 114.1, 112.2 (PyC-3/PyC-4); 84.5 (C−CH_3); 27.2 (CH_3). UV (CH_3CN) λ_{max} 419 nm.

2,5-Diphenylpyrrole (7a). After thermolysis of neat **5a** at 190 °C under vacuum during 15 min, pure **7a** was obtained in quantitative yield. ^{1}H NMR (THF-d_8) δ 10.40 (s, 1H, H-1); 7.63 (dd, J = 7.4 and 1.1 Hz, 4H, *o*-Ph); 7.31 (t, J = 7.4 Hz, 4H, *m*-Ph); 7.12 (tt, J = 7.4 and 1.1 Hz, 2H, *p*-Ph); 6.51 (d, J = 2.5 Hz, 2H, H-3,4). UV (CH_3CN) λ_{max} 328 nm.

5,5′-Diphenyl-2,2′-bipyrrole (7b). After thermolysis of neat **5b** at 190 °C under vacuum during 15 min, pure **7b** was obtained in quantitative yield. ^{1}H NMR (THF-d_8) δ 10.33 (s, 2H, H-1,1′); 7.56 (dd, J = 7.4 and 1.1 Hz, 4H, *o*-Ph); 7.28 (t, J = 7.4 Hz, 4H, *m*-Ph); 7.08 (tt, J = 7.4 and 1.1 Hz, 2H, *p*-Ph); 6.48 (dd, J = 3.5 and 2.5 Hz, 2H, H-3,3′/H-4,4′); 6.37 (dd, J = 3.5 and 2.5 Hz, 2H, H-3,3′/H-4,4′). UV (CH_3CN) λ_{max} 360 nm.

5,5″-Diphenyl-2,2′:5′,2″-terpyrrole (7c). After thermolysis of neat **5c** at 190 °C under vacuum during 15 min, pure **7c** was obtained in quantitative yield. ^{1}H NMR (THF-d_8) δ 10.23 (s, 2H, H-1,1″); 10.12 (s, 1H, H-1′); 7.55 (m, 4H, *o*-Ph); 7.28 (m, 4H, *m*-Ph); 7.08 (m, 2H, *p*-Ph); 6.47 (m, 2H, H-4,4″); 6.31 (m, 4H, H-3,3″,3′,4′). UV (CH_3CN) λ_{max} 374 nm.

5,5‴-Diphenyl-2,2′:5′,2″:5″,2‴-quaterpyrrole (7d). After thermolysis of neat **5d** at 190 °C under vacuum during 15 min, pure **7d** was obtained in quantitative yield. ^{1}H NMR (THF-d_8) δ 10.21 (s, 2H, H-1,1‴); 10.09 (s, 2H, H-1′,1″); 7.56 (m, 4H, *o*-Ph); 7.28 (m, 4H, *m*-Ph); 7.08 (m, 2H, *p*-Ph); 6.48 (m, 2H, H-4,4‴); 6.28 (m, 4H, H-3,3′,3″,3‴,4′,4″). UV (CH_3CN) λ_{max} 373 nm.

2,5-Bis(5-phenyl-2-pyrrolyl)thiophene (8a). After thermolysis of neat **6a** at 190 °C under vacuum during 15 min, pure **8a** was obtained in quantitative yield. ^{1}H NMR (THF-d_8) δ 10.53 (s, 2H, H-1′); 7.62 (dd, J = 7.4 and 1.1 Hz, 4H, *o*-Ph); 7.32 (t, J = 7.4 Hz, 4H, *m*-Ph); 7.13 (tt, J = 7.4 and 1.1 Hz, 2H, *p*-Ph); 7.06 (s, 2H, ThH-3,4); 6.51 (dd, J = 3.5 and 2.5 Hz, 2H, PyH-3/PyH-4); 6.40 (dd, J = 3.5 and 2.5 Hz, 2H, PyH-3/PyH-4). UV (CH_3CN) λ_{max} 390 nm.

5,5′-Bis(5-phenyl-2-pyrrolyl)-2,2′-bithiophene (8b). After thermolysis of neat **6b** at 190 °C under vacuum during 15 min, pure **8b** was obtained in quantitative yield. ^{1}H NMR (THF-d_8) δ 10.55 (s, 2H, NH); 7.62 (dd, J = 7.4 and 1.1 Hz, 4H, *o*-Ph); 7.31 (t, J = 7.4 Hz, 4H, *m*-Ph); 7.13 (tt, J = 7.4 and 1.1 Hz, 2H, *p*-Ph); 7.13 (d, J = 3.8 Hz, 2H, ThH-3/ThH-4); 7.09 (d, J = 3.8 Hz, 2H, ThH-3/ThH-4); 6.50 (dd, J = 3.5 and 2.5 Hz, 2H, PyH-3/PyH-4); 6.40 (dd, J = 3.5 and 2.5 Hz, 2H, PyH-3/PyH-4). UV (CH_3CN) λ_{max} 427 nm.

5,5″-Bis(5-phenyl-2-pyrrolyl)-2,2′:5′,2″-terthiophene (8c). After thermolysis of neat **6c** at 190 °C under vacuum during 15 min, pure **8c** was obtained in quantitative yield. ^{1}H NMR (THF-d_8) δ 10.57 (s, 2H, NH); 7.62 (dd, J = 7.4, 1.1 Hz, 4H, *o*-Ph); 7.32 (t, J = 7.4 Hz, 4H, *m*-Ph); 7.13 (m, 8H, *p*-Ph/ThH-3′,4′/ThH-3,3″/ThH-4,4″); 6.51 (dd, J = 3.5 and 2.5 Hz, 2H, PyH-3/PyH-4); 6.42 (dd, J = 3.5 and 2.5 Hz, PyH-3/PyH-4). UV (CH_3CN) λ_{max} 431 nm.

Acknowledgment. We thank Ms. L. Verhoeven for assistance in preparing the oligomers. Philips Research is gratefully acknowledged for an unrestricted research grant.

CM950332G